IOSR Journal of Mechanical and Civil Engineering (IOSR-JMCE)
e-ISSN: 2278-1684,p-ISSN: 2320-334X, Volume 12, Issue 5 Ver. II (Sep. - Oct. 2015), PP 68-74
www.iosrjournals.org

Study On Fatigue Crack Growth Behavior Of Aluminum Alloy In The Presence Of Notch: An FEA Approach

Mahantesh. Matur[1], V. Krishnan[2], P. Dinesh[1]
[1](*Department of Mechanical Engineering, M.S.Ramaiah Institute of Technology, Bangalore / VTU, India)*
[2](*Department of Mechanical Engineering, Sir M. Visveshwaraya Institute of Technology, Bangalore / VTU, India)*

Abstract: *Motivated with the functioning of pressure cylinders and their failures due to the presence of initial flaws, an arc shaped specimen with inner surface notch is used as the theme of the present fatigue crack growth study. Stress intensity factor (SIF) values obtained by the numerical simulation for the single edge notch bend (SENB) specimen show a good agreement with the results obtained by photo elastic technique and hence using the same numerical simulation based finite element analysis (FEA) technique, an influence of presence of notch on the fatigue life of aluminum specimen was investigated by the numerical simulation and compared with experimental results. Test samples and testing methods utilized for the present study are in accordance with American Society for Testing and Materials (ASTM) standards. Outcome of the study shows the dependency of crack propagation on the stress intensity range.*

Keywords: *Aluminum, Arc shaped specimen, ASTM, Fatigue crack growth, FEA*

I. Introduction

Generally components are designed so as to avoid yielding at the worst loaded point. Safety against yield or failure of a component is considered to be the basic requirement of any design. Hence designers give more importance to design featuring, notches[7], joints[8], complexity of specimen geometry[4] and groves[5,6] to minimize the stresses that leads to premature failure of the components.

Components fail , when load applied is beyond the yield strength of the material. However it has been found that often structures fail , even when load is well within the yield stress. Thus we can note that design of a component based completely upon avoiding yielding is not adequate in certain cases such as in fatigue cases.

Fracture mechanics has become a perfect tool to deliver a useful methodology to compensate the inadequacies of conventional design concepts. The conventional design criteria are based on tensile strength , yield strength and buckling stress. These criteria are useful for several engineering applications , but they are insufficient when there is a crack in a structure. Hence integrity of many engineering structures are in jeopardy by the presence of these initial cracks. Even though the design may appear to be safe , but structure may fail due to aggravation of secondary cracks under same or low cyclic loads. These secondary cracks may grow either from the free surface or from the initial geometrical features such as notches. Hence it is essential to address the problem of notch under fatigue loads and consequent failure of the structures. Thus objective of present study is to study the Fatigue crack growth (FCG) characteristics of aluminum alloy specimen with a notch .

The crack that is likely to grow under given loading condition can be analyzed through several methods such as stress method, displacement or energy method[2,3]. For surface crack problems, many analyses have been reported. T. Nishioka and S. N. Atluri's [13] three-dimensional Alternating method; In this method, in conjunction with the finite element method , the analytical solution was used for the analyses of semielliptical surface flaws in pressurized cylinders. Using FEA, an uncracked cylinder under external load, was solved. Solution thus obtained were used to calculate the stress at the location of the crack. Then using the analytical solution in terms of coefficients, stress intensity factor were obtained.

German et al's [14] line-spring method; In this method, the surface cracked configuration was idealized as through- the thickness crack and discretized using plate/ shell elements with a series of line spring elements with the crack faces. The line-spring model was applied for the analysis of surface cracks in plates using ADINA software.

Raju, I.S., and Newman, J.C., Jr, [16] proposed finite element method; Crack opening displacement approach to extract mixed mode SIF(s) has one disadvantage in 3D crack problems that a state of plane strain or plane stress must be assumed initially. To circumvent this problem Raju and Newman proposed the nodal force method and applied for semicircular surface crack in finite thickness plate in remote tension.

Bernard Gross et al's [18] boundary collocation method; A boundary-value- collocation procedure was applied to the Williams stress function to determine values of the stress-intensity factor K for single-edge cracks in rectangular- section specimens subjected to three-point bending. The results are in terms of dimensionless quantity relating, specimen thickness, width and bending moment.

J. E. Srawley's[19] photoelastic local collocation method; In this method to determine the SIF, a series of photoelastic experiments was performed on a model of SEN, three point bending specimen. To determine the SIF, classical fracture mechanics approach was followed .

The boundary collocation analysis yielded much more information than the photo elastic analysis but the photoelastic method provides a cost effective alternative to the numerical analysis.

Aluminum 6061 alloy (hence forth read as AL 6061) as used for the present study has many applications due to its high strength to weight ratio. Basically in automotive sector, aerospace and in manufacture of pressure vessels. This material can be easily heat treated to improve the mechanical properties of the components under service[1]. In the present study it is proposed to study the crack propagation in an arc shaped tension (AT) specimen made up of AL 6061, by conducting FCG test. The result of FCG test gives SIF range (ΔK) and the number of cycles for failure. The resulting ΔK is also obtained by using FE technique, where SIF is extracted by the quarter point method. For the present problem, a stress approach is followed to analyze a crack growth on curved surface at room temperature under mechanical loading. In this approach , there is a need to account for the large amount of stresses, that are developed in the vicinity of a crack tip requiring fine mesh at the crack tip for determining the SIF.

II. Fatigue Crack Growth Test Details

In the following paragraphs, details of the material, specimen geometry and test procedure employed in studying the fatigue crack growth behaviour of AL 6061 in the presence of notch are presented.

2.1 Specimen details

For the present study, specimen made up of AL 6061 with the composition as shown in TABLE 1 has been used.

Table 1. Typical composition of AL 6061 (Weight %)

Content	**CU**	**Mg**	**Si**	**Fe**	**Mn**	**Al** Rest
Percentage	0.066	0.72	0.876	0.162	0.54	
Content	**Ni**	**Pb**	**Sn**	**Ti**	**Zn**	
Percentage	<0.05	0.024	0.009	0.025	0.009	

An AL 6061 extruded circular bar of 160 mm diameter and 150 mm length is used for preparing the specimen. An AT specimen geometry as shown in Fig. 1 is produced from these extruded circular bar. After the turning operation , the round bar is subjected to boring operation to obtain the rings. Grinding operation is carried out to obtain good surface finish before machining with the help of wire EDM (Electric Discharge machining) and the stages of preparation are as shown in Fig. 2 (a-d). Specimen geometry with notch of CR orientation as per the crack plane orientation code suggested by ASTM E-399 is used in the present study. The notch geometry is 4 mm in length with nose radius of 0.25 mm. Using wire EDM, the specimen and notch as shown in Fig. 2 (c and d) were machined.

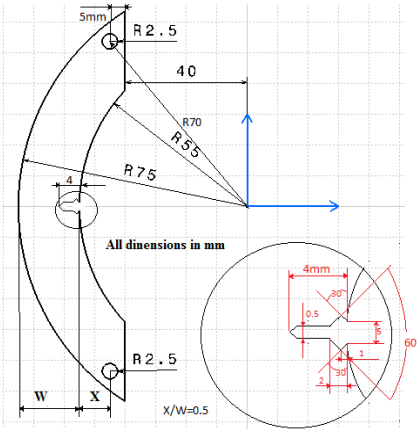

figure. 1 Specimen geometry

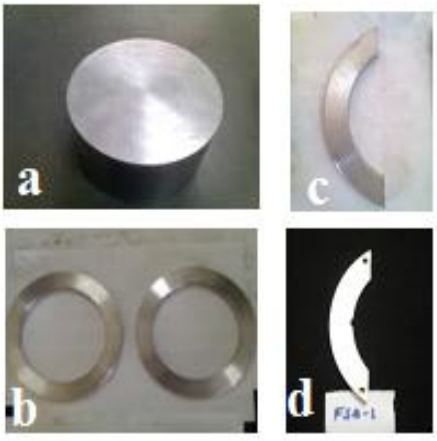

figure. 2 (a – d) Stages of specimen preparation

Fig. 3 shows the experimental set up , where in the specimen is held between the tension testing clevis suitable for testing arc-shaped specimen. To monitor the crack growth, displacement gauge is mounted at the mouth of the notch where a small opening is provided as shown in fig. 1. The scanning electron microscope

image of the notch as shown in Fig. 4 is taken, before the failure of the specimen to observe the grain orientation. From the image it is seen that the grain orientation is along the loading direction.

figure. 3 Experimental setup

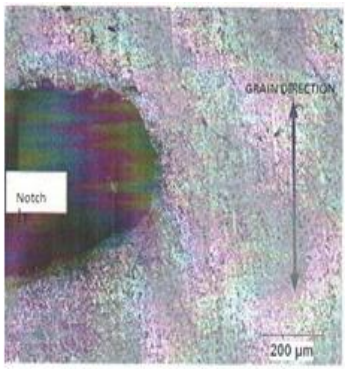

figure. 4 Scanning electron microscope image of the notch

2.2 Test procedure

Fatigue crack growth test has been carried out as per the procedure recommended by ASTM 647-08 with the help of experimental setup as shown in Fig. 3. Specification of the Fatigue testing machine, in brief is as follows; Servo controlled hydraulic actuator with ±50 to 100 mm stroke. Basically the machine is Bi-01-100-2CTT series model with table-top-test systems equipped with T-slotted base. The frame, controls and display are located on the table and provide the flexibility to perform static and dynamic tests. Important features of model are, cyclic frequency of 0- 100 Hz and load capacity range of 5-50 KN.

Using the above said machine, specimen was subjected to a constant amplitude cyclic loading with a sinusoidal wave form at a frequency of 10 Hz and load ratio R=0.3 at room temperature. The load range ΔP= 2.31 kN and the ratio X/ W of 0.5 is used in the present study, where X is the distance of loading and W is width of the specimen as shown in Fig. 1. The resulting crack propagation in the width direction of the specimen is recorded with the help of crack opening displacement (COD) gauge.

III. Numerical Simulation Of The AT Specimen FCG Test

To establish a correct Finite Element (FE) procedure for determining ΔK by numerical simulation of AT specimen FCG test, a 3 point SENB was considered and the normalized SIF versus relative crack length was plotted and compared with published results which established the correctness of the procedure to be followed for FE simulation. This procedure has been later applied to the AT specimen using ANSYS software to simulate the FCG test discussed in the previous section.

3.1 Simulation and validation of FE procedure

Specimen geometry of the SENB specimen for the test is as suggested by ASTM E1820 (ASTM, 2013), with width equal to $1/4^{th}$ of the span. As per standard, normalized SIF , f(a/W) was calculated by making use of SIF values, so obtained through FE simulation. A plot of normalized SIF versus relative crack length, thus constructed compares well with the plot as obtained by other authors [19] as shown in Fig.5.

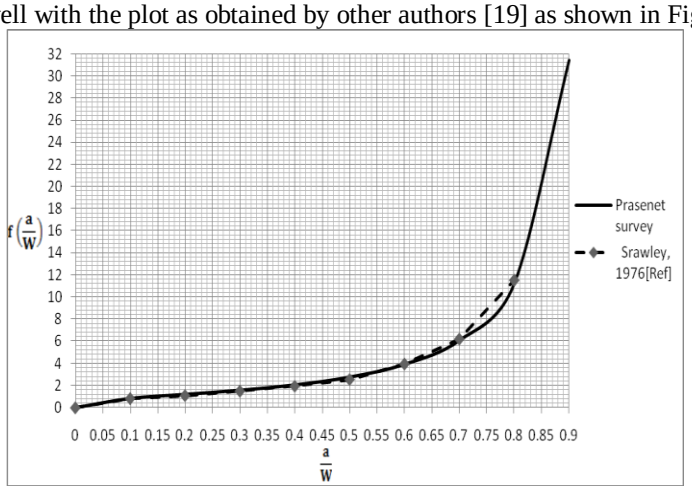

figure. 5 Characteristic relationship between Normalized SIF versus relative crack length

This comparison with published results establishes the FE procedure to be applied in the present study in determining ΔK of a curved specimen (AT specimen) obtained through FCG test .

3.2 Analysis of AT specimen

After the validation of FE procedure for simulation of SENB test in the previous section, the same is applied to analyse an AT specimen for plain strain conditions. The FE model was meshed with Brick 20 node 186 elements. Modulus of elasticity and Poisson's ratio of 68.9 GPa and 0.33 respectively are used as material properties. To obtain crack tip stress fields at the key point, a sufficiently fine mesh of 0.05 mm [9, 10] was incorporated as shown in Fig. 6a. In this study the total number of elements created were 16980. At the lower hole of the specimen all DOF were specified to be zero and the maximum tensile load of 3300 N is applied at the upper hole of the specimen as shown in Fig. 6b. After obtaining the stress distribution(as shown in Fig. 6c), (K_I)max is extracted for the maximum loading and the process is repeated for minimum load of 990 N to obtain SIF (K_I)min.

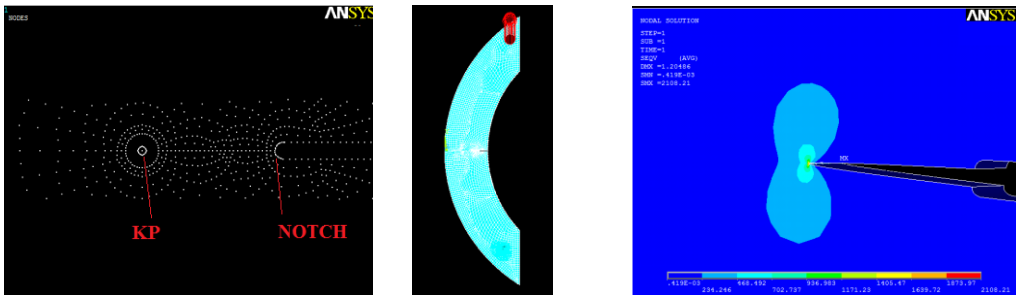

a b c

figure. 6 Finite element a) mesh at the notch. b) load and constrain c) nodal solution

The process is continued up to the stage when (K_I)max reaches (K_{IC}), where K_{IC} is critical stress intensity of the AL 6061. Using equation : $da / dN = C (\Delta K)^m$ (1) and the Paris constants C and m obtained from the experiments as in TABLE 2, fatigue crack growth rate is computed. The number of cycles required for the crack propagation up to the failure is calculated using the integral form as reported[11,12] : $\int_{ai}^{af} \frac{da}{C(\Delta K)^m}$ (2).

Number of stress cycles for crack initiation has not been included in the total life cycle calculation of the specimen under consideration.

IV. Results And Discussion

The following paragraph discus the results obtained from the FCG test and the Numerical simulation of the same.

4.1 FCG test results

From the FCG testing machine, the plot of crack length versus number of stress cycles is obtained and is as shown in Fig. 7. The plot of crack growth rate da / dN as a function of stress intensity factor range (ΔK) is plotted from the test results and is as shown in Fig. 8. From this plot, the Paris constants[12] were determined using curve fitting technique. TABLE 2 shows the values of **C** and **m** for different values of correlation factor R^2 and the highest value of correlation factor determines the value of Paris constants for being used for the numerical solution. These values of **C** and **m** are in good agreement with published results [15] for the AL 6061.

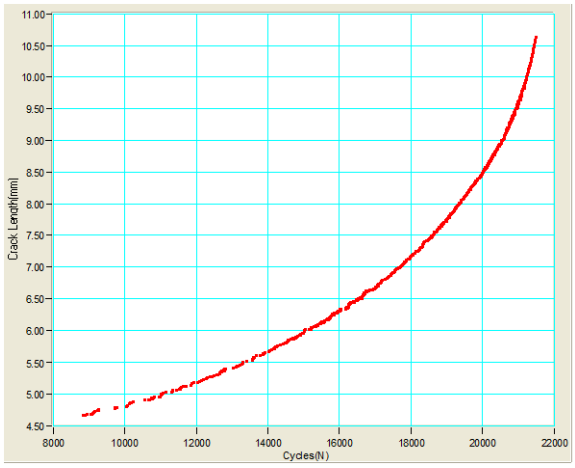

figure. 7 Crack growth curve

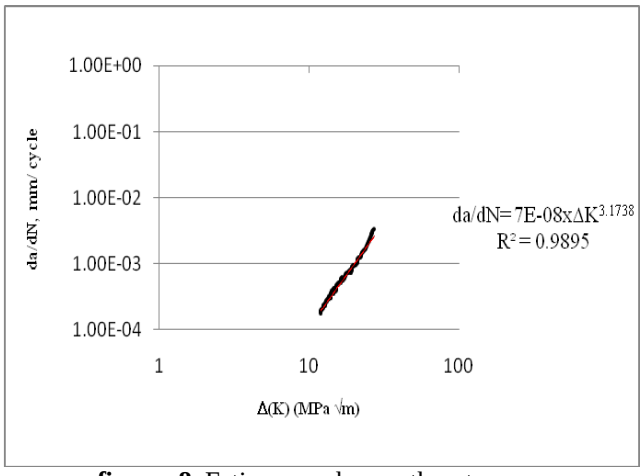

figure. 8 Fatigue crack growth rate curve

From the results, it's been observed that, fatigue crack growth behavior depends mainly on two stress intensity fracture mechanics parameters, i.e. ΔK and (K_I) max. Stress intensity range, explains the fatigue damage behavior of the material, whereas maximum SIF explains the crack tip widening under the applied load.

Table. 2 Paris constants

Material	da/dN = C $(\Delta K)^m$		R^2
	C	m	
Al- 6061	**7.00E-08**	**3.17**	**0.9895**
Al- 6061	1.00E-07	3.03	0.9883
Al- 6061	6.00E-10	4.68	0.9845
Al- 6061	7.00E-18	11.47	0.9819
Al- 6061	1.00E-16	10.5	0.9186

Fig. 9 shows the plot of stress intensity range versus crack length obtained from FCG test and numerical simulation. Numerical simulation results are in close agreement with test results. The results obtained from the experiment reveals that, there exist some ΔK that helps in the nucleation of crack and at (K_I) max of 17.5 MPa√m, crack has grown by 1 mm. Material weakening prolongs as the repetitive load continues on the material, leading to the fatigue damage of 21.28 MPa√m. By the time, stable crack resistance of the material have been reached, as crack grows to 5 mm from the notch.

This plot also establishes the fact that, on loading the crack grows with increase in stress levels and this shows the dependency of the crack propagation on the stress intensity range.

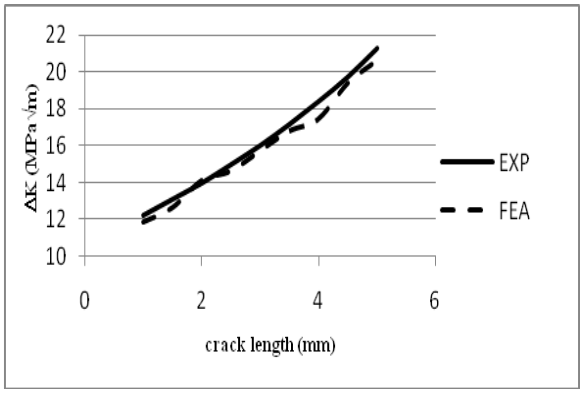

a

figure. 9 stress intensity range comparison.

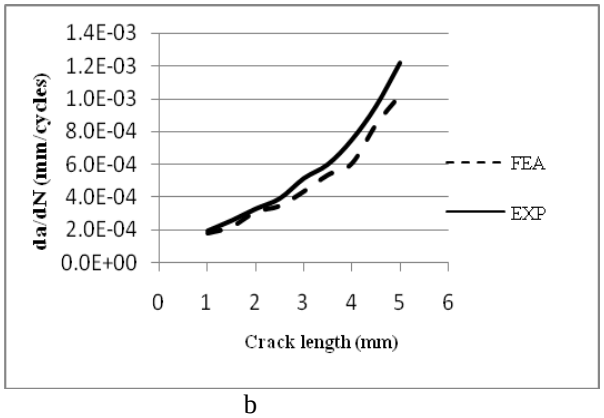

b

figure. 10 crack growth rate curve comparison

Fig. 10 shows the plot of crack growth rate versus crack length obtained from the experiment and Numerical simulation. Numerical simulation results in terms of crack growth rate as obtained using equation (1) are in close agreement with experimental results with small deviation. This plot shows that, crack grows at faster rate, as Stress Intensity Factor starts reaching the maximum value i.e., (K_I) max. The range of the stress cycles

required to grow the crack from 2 to 5 mm under stable crack growth is of the order of 3.31 x 10^{-4} to 1 x 10^{-3}. Beyond this, as SIF (K_I) increases, the plastic zone size increases compared to the crack length and material fails with little stress cycles.

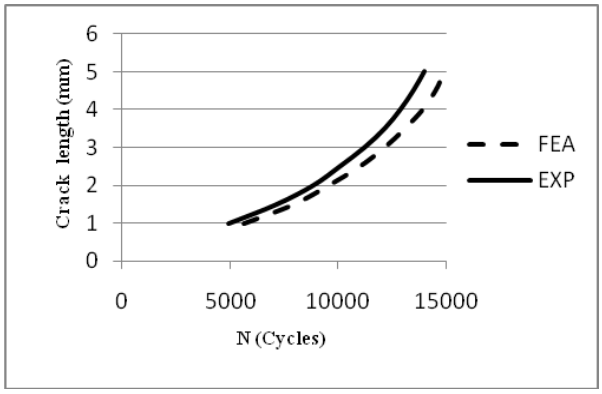

figure. 11 crack growth curve comparison.

Fig. 11 shows the plot of crack length versus number of stress cycles obtained from experiment and Numerical results. It shows that, the number of cycles obtained from experiment, to propagate the crack from the initial notch, up to the failure of the material, is 13,989 cycles . Whereas FEA results as obtained using equation (2) , shown the same trend, but failed to 14,888 cycles, with variation of 6%. Note that, as mentioned above, the number of stress cycles required for the initiation of the crack from the notch is not considered.

2.3 Analysis of specimen after failure

Finite Element result and failed specimen details are as shown in Fig. 12 (a and b). We observed that the plastic failure zones of FE and failed specimen are almost have same crack pattern.

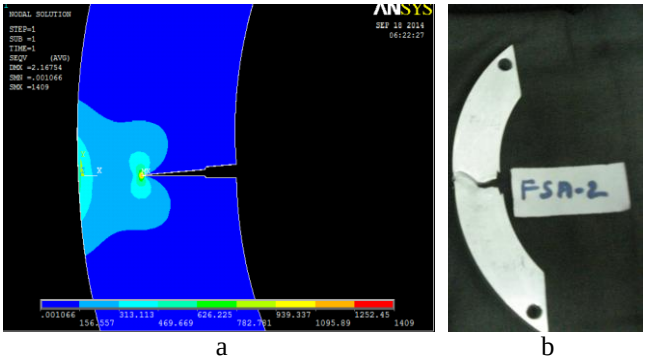

a b

figure. 12 fractured specimen as observed through a. FEA b. experiment

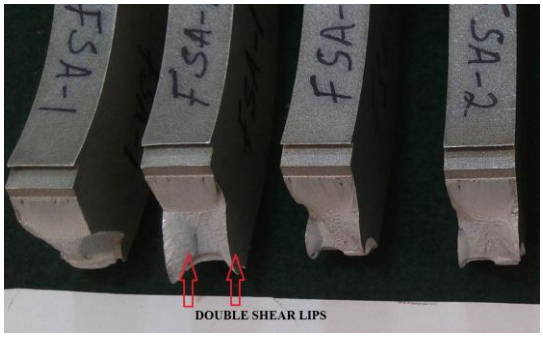

figure. 13 Double Shear lips

Fig. 13 shows the fractured specimen having double shear lips so formed during crack propagation and the ultimate failure. The crack propagation pattern in AL 6061, are due to the changes in the crack surface from flat to slant at higher crack growth rates or ΔK levels as reported [19]. Shear lip initiates at the plate surface and grows as the stress intensity range increases. Shear lip formation is due to the propagation of crack along the slip plane, as the slip possibility near 45^0 with the specimen fracture surface is maximum . The start of the shear lip can be found in the da /dN versus ΔK diagram as shown in Fig. 8 of a constant load amplitude test as a change of slope in the crack growth curve takes place[20]. Also the da/dN need to be high enough to cause the formation of inclined surface.

V. Conclusion

Experimental and Numerical simulation of fatigue crack growth in an AT specimen of AL-6061 as fabricated with an initial notch has been presented. As not much work in the literature on studies of crack propagation in curved surfaces as encountered in pressure vessels, this study gains importance for such a crack propagation in AL-6061. This study establishes the fact that, crack initiation and propagation start from regions of high stress levels and dependency of SIF range on crack growth during fatigue loading. The crack propagation pattern in aluminum alloys, are due to the changes in the crack surface from flat to slant at higher

crack growth rates that leads to the formation of shear lips. This study has also established a Finite element method procedure for numerical solution of a FCG test of an AT specimen. This study will help in design of pressure vessels and cylinders based on the concept of pre-existence of flaws.

References

[1] J. Andrea Carpinteri, Roerto Brighenti, and Sabrina Vantadori, Notched double curvature shells with cracks under pulsating internal pressure, International Journal of Pressure Vessels and Piping, 86, 2009, 443-453.

[2] M. Adeel, Study on Damage Tolerance Behavior of Integrally stiffened panels and conventional stiffened panel, Proceedings of world academy of science , engineering and technology, 35, November-2008, ISSN 2070-3740.

[3] C.Q.Li and S.T.Yang , Stress Intensity Factor for high aspect ratio semi elliptical internal surface cracks in pipes, International Journal of Pressure Vessels and piping, 96-97, 2012, pg 13-23.

[4] Y. Kim, Y. J. Chao , M.J.Pechersky and M.J. Morgan, C-specimen fracture Toughness Testing ; Effect of side grooves and η – factor, Journal of Pressure Vessels Technology ,126, ASME, August 2004, 293-299.

[5] Y.Tkach, F.M. Burdekin, A three dimensional analysis of fracture mechanics test pieces of different geometries- part I Stress state ahead of the crack tip, International Journal of Pressure Vessels and Piping, 93-94, 2012, 42-40.

[6] Broek. D, Elementary engineering fracture mechanics (Dordrecht: Martinus Nijhoff publication, 1982).

[7] Barsom. J. M and Rolfe. S. T, Fracture and fatigue control in structures (Englewood cliffs, Newjersey :Prentice-Hall, Inc, 1987).

[8] T. Nishioka and S. N. Atluri, Analysis of surface flaw in pressure vessels by a new 3-Dimensional Alternating method , Journal of pressure vessel technology, 104, ASME, 1992, 299-307.

[9] German. M. D, Kumar. V and Delorenzi. H. G, Analysis of Surface Cracks and Plates Using a Line Spring Model and ADINA, Computers and Structures, 17, 1983, 881-890.

[10] Raju. I.S, and Newman. J.C. Jr, Stress Intensity Factor for Wide Range of Semi-Elliptical Surface Cracks in Finite thickness Plates, Engineering Fracture Mechanics, 11, 1979, 817-829.

[11] Bernard Gross and John. E. Srawley, Stress intensity factors for three point bend specimens by Boundary collocation, National Aeronautics and Space Administration (NASA)Technical Note, TN D- 3092, NASA, Washington, D.C, December 1965, 1-13.

[12] Srawley. J. E, Wide Range SIF Expressions for ASTM Standard E-399, Fracture Toughness Test Specimens, International Journal of Fracture, 12(3), June 1976, 475-486.

[13] Gladman T, Precipitation hardening in metals, Material Science and Technology, 15, 1999, 30-36.

[14] S. Stoychev and D. Kujawski, Crack tip stresses and their effect on Stress Intensity Factor for crack propagation, Engineering Fracture Mechanics, 75, 2008, 2469- 2479.

[15] I. Salam, M. Abid, M. A. Malik, Crack growth prediction in a thick cylinder under fatigue loading-an FEA. International Journal of Systems Applications, Engineering and Development, 3(1), 2007, 51-55.

[16] Shine U P, EMS Nair, Fatigue failure of structural Steel- analysis using fracture mechanics, World academy of science engineering and Technology, 46, 2008, 616-619.

[17] P. C. Paris and F. Erdogan, A Critical Analysis of Crack Propagation Laws, Trans. ASME, Journal of Basic Engineering, D85, 1963, 528-534.

[18] R.R.Ambriz.et. al, Fatigue crack growth under a constant amplitude loading of Aluminum -6061-T6 welds obtained by MIEA technique, Science and Technology of Welding and Joining, 15(6), 2010, 514-521.

[19] J. Zuidema.et. al, Shear lips on fatigue fracture surfaces of Aluminum alloy, Fatigue Fracture Engineering Material Structure, 28, 2005, 159-167.

[20] J. J. McGowan and H. W. Liu, The role of three dimensional effects in constant amplitude fatigue crack growth testing, Journal of Engineering Materials and Technology, 102(4), 1980, 341-346.